ResearchGate

See discussions, stats, and author profiles for this publication at: https://www.researchgate.net/publication/304008971

Land use/land cover change and driving effects of water environment system in Dunhuang Basin, northwestern China

Article *in* Environmental Earth Sciences · June 2016

DOI: 10.1007/s12665-016-5809-9

CITATIONS
7

READS
146

6 authors, including:

Weitao Chen
China University of Geosciences
28 PUBLICATIONS **474** CITATIONS

SEE PROFILE

Yanxin Wang
China University of Geosciences
381 PUBLICATIONS **9,420** CITATIONS

SEE PROFILE

Xianju Li
China University of Geosciences
21 PUBLICATIONS **460** CITATIONS

SEE PROFILE

Some of the authors of this publication are also working on these related projects:

neural networks algorithm View project

High arsenic groundwater in the Jianghan Plain View project

All content following this page was uploaded by Weitao Chen on 20 July 2016.

The user has requested enhancement of the downloaded file.

Environ Earth Sci (2016) 75:1027
DOI 10.1007/s12665-016-5809-9

ORIGINAL ARTICLE

Land use/land cover change and driving effects of water environment system in Dunhuang Basin, northwestern China

Weitao Chen[1,2] · Yanxin Wang[3] · Xianju Li[4] · Yi Zou[1] · Yiwei Liao[5] · Juncang Yang[6]

Received: 13 August 2015 / Accepted: 1 June 2016 / Published online: 16 June 2016
© Springer-Verlag Berlin Heidelberg 2016

Abstract The Dunhuang Basin, located in northwestern China, is famous for its oases and geological remains. However, some problems of the eco-environment have raised public concern in recent decades. Land use/land cover change (LUCC) has been considered essential reference for studying eco-environment across the world. In the present study, the land use/land cover was divided into natural water, salt marshes, *Aeluropus littoralis*, natural vegetation, barren land, and desertified land. The LUCC was analyzed using four temporal Landsat images (from around 1975, 1990, 2000, 2010, respectively) and RapidEye images in 2010. Firstly, vegetation degeneration is the most serious problem, and 926.74 km^2 turned into bare land in the past 35 years. The total area of bare land increased mainly occurred during 1975–1990. The area of desertified land increased rapidly from 2000 to 2010. Secondly, wetlands have experienced extreme shrinking; some areas degenerated into salt marshes, subsequently vanished. Salt marsh areas have been continually decreasing and gradually degenerating into saline and alkaline lands and bare land. In relation to the driving forces of LUCC, according to collected data and interpretation results by remote sensing images, the surface water environment is destructive due to three reservoirs impede surface water supplementation to the soil and natural vegetation. In addition, excessive pumping of groundwater occurred in the study area. Based on the local soil profiles of vadose zones and dynamic change of groundwater level, the groundwater flow system is another key factor, which developed along with the spatial distribution of groundwater recharge, runoff, and discharge conditions. Furthermore, large-scale activities connected to the reclamation of commercial farmlands have also promoted the LUCC.

Keywords Land use/land cover changes (LUCC) · Remote sensing · Machine learning algorithm · Dunhuang Basin · Groundwater · Landsat · RapidEye

✉ Weitao Chen
wtchen@cug.edfyhu.cn

1 Faculty of Computer Science and Hubei Key Laboratory of Intelligent Geo-Information Processing, China University of Geosciences, Wuhan 430074, China

2 Faculty of Geo-Information Science and Earth Observation, University of Twente, 7500AE Enschede, The Netherlands

3 School of Environment Studies and State Key Laboratory of Biogeology and Environmental Geology, China University of Geosciences, Wuhan 430074, China

4 Faculty of Information Engineering, China University of Geosciences, Wuhan 430074, China

5 School of Electrical and Electronic Engineering, Huazhong University of Science and Technology, Wuhan 430074, China

6 Gansu Province Institute of Geological Environmental Monitoring, Lanzhou 730050, China

Introduction

Problems in eco-environment, especially in arid regions, have increasingly raised public concern across the world. Arid and semiarid areas are widely distributed in China, but are rich in wetland and vegetation resources. The arid climate, complex geological conditions, and increased human activity have created eco-environment problems, such as lack of water resources, desertification, salinization, and biogeochemical endemic diseases (Tang and Lin 1995). The Dunhuang Basin is located on the lower reach of the SuLe River, situated on the western end of northwestern China's Hexi Corridor. The Basin is bounded by

the Mingsha, Sanwei, and Beijie Mountains to the southeast, the Mazong and Bei Mountains to the north and the desert to the west. The Dunhuang Basin boundary is composed of a series of faults. This region is famous for the channels of the ancient Silk Road. The MoGao Grottoes are considered a World Heritage Site, both the YangGuan and the Han Great Wall are famous historic cultural landmarks, and the Crescent Moon Spring and the YaDan landform are both National Geological Parks. These unusual natural landscapes attract a great number of visitors each year. However, because the Lop Nor Lake has dried up, the western Dunhuang Basin's West Lake National Reserve has been playing an increasingly vital role in protecting the eco-environment of Dunhuang City. Furthermore, it is now becoming the last barrier protecting the ecological safety of northwestern China and improving the regional climate conditions because it is actually threatened by the Takalamagan and Tumutage deserts. In order to recover the eco-environment in the Dunhuang Basin, the national water resources project, "Haerteng River-to-Dang River water diversion," was conducted in 2015.

In arid regions, land use/land cover (LULC) represents important information on the natural landscape and human activity on the earth's surface (Gong et al. 2011). Land use/land cover change (LUCC) has substantial impacts on a vast array of environmental systems, including hydrological and ecological, and is also a key data input for a wide number of climate and land surface models (Foley et al. 2005). Meanwhile, LUCC has increasingly become a core part of the research related to global environmental change, including monitoring and understanding the ongoing processes of deforestation and desertification (de Freitas et al. 2013; Hüttich et al. 2011; Li et al. 2013; Lira et al. 2012; Liu and Deng 2010; Pérez-Hoyos et al. 2012; Turner et al. 2007; Zhao et al. 2013). It has been noted that LUCC could be considered one of the references for studying eco-environment problems (Li et al. 2013; Zhao et al. 2013; Ni and Shao 2013). Satellite remote sensing data, which provide large-scale and up-to-date information on earth surface conditions, can be used for accurate and efficient LUCC research at a variety of spatial scales (Gong et al. 2011). Thus, considerable effort has been directed to the derivation of LUCC from remote sensing (Foody 2010).

Over the last two decades, LUCC at the national and regional scale in China has led to increased analysis of the processes, driving forces, impacts, and future trends by using long time series of Landsat data (Sun et al. 2009). The sandy desertification trends in the Sule River Basin have been assessed using the vegetation index derived from four temporal Landsat images from 1978 to 2010, and the results indicated that climate and human activity, such as inappropriate land use, were the driving forces of desertification (Song et al. 2014). In addition, the impact of LUCC on groundwater depletion in the Dunhuang oasis has been quantified using Landsat data of 1987,1990, 1996, 2001, and 2007 (Zhang et al. 2014). The evolution and recharge of groundwater and hydrogeological and hydrogeochemical control of groundwater salinity in the Quaternary aquifer beneath Dunhuang Basin have been investigated using chemical indicators, stable isotopes, and radiocarbon data (Ma et al. 2013; Sun et al. 2015). As yet, little research has been conducted on the LUCC and driving effects of water environment system (WES) that considers the entire Dunhuang Basin. Instead, much of the research thus far has focused on individual factors or processes, such as desertification (Wang 2009), water resources, and visual simulations of groundwater (Sang 2006; Zhang et al. 2003).

The objectives of this paper are as follows: (1) to first determine the LUCC using four temporal Landsat datasets (1965, 1990, 2000, 2010) and RapidEye images in 2010 and articulate the key eco-environment problems in the Dunhuang Basin and (2) to analyze the driving effects of the WES on LUCC of the Dunhuang Basin. The achievements were expected to contribute to providing beneficial measurements to restore eco-environment of the Dunhuang Basin.

Geological and hydrogeological background

General setting

The Dunhuang Basin stretches westward to the Guazhou irrigation area and eastward to the border of the XinJiang Uygur Autonomous Region (refer to Fig. 1). Because the Gobi Desert did not change during the present study period, the area was interpreted artificially based on the RapidEye images listed in Sect. 3. The area that does not include the Gobi Desert, covering a total area of 3608.09 km^2, was selected for LUCC classification. The southern border of this study area is Sanwei Mountain, and the northern border comprises low mountains and hills.

There are various and complicated landscapes of highlands, plains, and stone deserts in the study area, which can be divided into three types of geomorphology: constructional eroded geomorphology, accumulated geomorphology, and eolian geomorphology.

The study area has an arid climate with the annual temperature difference of 34.1 °C and the perennial average rainfall of 40.1 mm, of which the evaporation capacity reaches 2417.19 mm. The area from Devil City to Yumen Pass has the least amount of rainfall and the greatest evaporation capacity. The 75 % of the total rainfall is concentrated in June, July, and August, with no uniform spatial distribution. In January, February, November, and

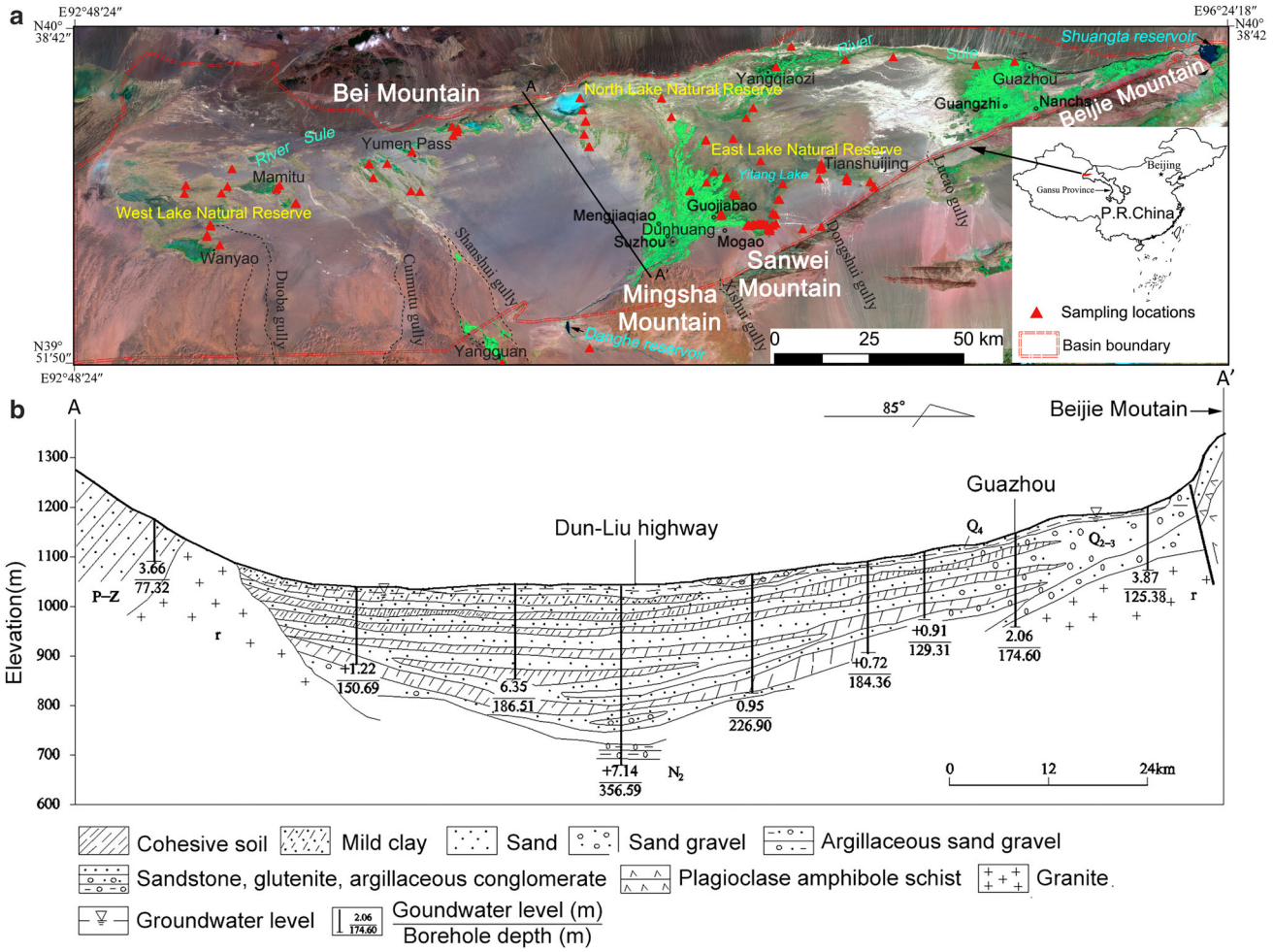

Fig. 1 Locations of the Dunhuang Basin with sampling locations and simplified geological cross section. The sampling locations include training samples and soil profile investigation

December, the rainfall is generally less than 6 % of the total rainfall. The evaporation capacity is the greatest from May to August. All of the weather stations in the study area report that the rainfall increases with elevation. The rainfall increases gradually from north to south, with a gradient of 5 mm rainfall/100 m elevation. Most rainfall occurs during the East Asian summer monsoon, during which time rainfall can exceed evapotranspiration, thus facilitating groundwater recharge.

Hydrogeology

The major outcropping strata in the mountain areas surrounding the basin are gneiss, quartzite, migmatite, limestone, and schist from the Presinian, Sinian, Cambrian, Ordovician–Silurian, and Permian periods, respectively. The regional basin-fill aquifer system is composed of thick Quaternary diluvial and alluvial sediments and some eolian and acustrine deposits. The porous Quaternary sediments are primarily composed of gravel, sand, silt, and clay (Fig. 1b). In the front area of the alluvial and diluvial fan in the south of the Dunhuang Basin, the aquifer is unconfined and composed of highly permeable cobbles, gravels, and sands with thicknesses between 200 and 400 m (Sun et al. 2015).

Data

In total, 12 scenes of Landsat imagery from 1975 (indicating hereby 1976, 1978, and 1973), 1990 (indicating hereby 1987, 1990, and 1991), 2000, and 2010 were used in this paper (Table 1). We mostly selected the imagery with autumn acquisition times for seasonal and phenophase uniformity. In addition, in order to improve the interpretation accuracy of LULC, RapidEye satellite data with 5 m spatial resolution acquired from July 14 to September 25, 2010, were used for the reference (Table 2).

From May to August in 2011, eco-hydrogeology survey in the Dunhuang Basin, including both LULC and local soil

Table 1 Characteristics of Landsat images used in the present study

Sensor	Imaging time	Path/row	Nominal spatial resolution (m)	Level
MSS	1976-10-05	147/32	79	1B
	1978-10-24	148/32	79	
	1973-12-25	149/32	79	
TM	2010-06-16	136/32	30	
	2010-07-09	137/32	30	
	2010-07-16	138/32	30	
	2000-08-31	136/32	30	
	2000-07-21	137/32	30	
	2000-07-12	138/32	30	
	1987-10-07	136/32	30	
	1990-09-04	137/32	30	
	1991-08-29	138/32	30	

profiles with the same locations, was carried out. Excavating artificial trenches were conducted in order to determine soil properties of vadose zones. The results revealed that the salt crust, silt, and various diameter sands were main features of soil profile.

Methods

Image preprocessing

In this study, geometric rectifications were first performed on the RapidEye images using 1/100,000 scale topographic maps. Then, the rectified RapidEye images were used to perform image-to-image rectification for all the Landsat images. The cubic convolution resampling method was used. All images were rectified to UTM Zone 46N, WGS 1984.

Accurate per-pixel registration of the four temporal Landsat images is essential for detecting LUCC (Rogan and Chen 2004). If the geometric registration is well done, the root-mean-square error (RMSE) between any intervals of data should not exceed 0.5 pixels (Lunetta and Elvidge 1998). The RMSE between every two images was actually less than 0.5 pixels in the present study, which is acceptable.

After the registration, the multiple images belonging to the same period were combined in a mosaic to form a single, seamless composite image. Then, the study area was extracted from the mosaic image.

Image classification and change detection

According to the LULC classification system developed by other researchers (de Freitas et al. 2013; Jensen and Cowen 1999; Seeber et al. 2010; Zhao et al. 2013), Landsat images are only suitable for level I land cover mapping. Thus, the following six types were determined as the LUCC classification scheme in the present study: natural water, salt marshes, *Aeluropus littoralis*, natural vegetation, barren land, and desertified land, as listed in Table 3.

The series of conventional classifiers, such as parallelepipeds, minimum distance, and maximum likelihood models, are well-developed and have long been used for remote sensing applications (Couturier et al. 2009; Gong et al. 2011; Hagner and Reese 2007). Other machine-learning classifiers have also been effectively applied to LULC mapping, such as artificial neural networks, machine-learning decision trees, genetic algorithms, and support vector machines (Atkinson and Tatnall 1997; Benediktsson et al. 1990; Fisher 2010; Gong et al. 2011; Stavrakoudis et al. 2010, 2011; Volpi et al. 2013). These classifiers have proven superior to the above-mentioned conventional classifiers, often recording overall accuracy improvements of 10–20 % (Rogan and Chen 2004; Volpi et al. 2013). In this study, four temporal Landsat images were independently classified using the artificial neural networks method in the ENVI 5.0 software; a brief introduction to the method be found in Benediktsson et al. (1990).

The training samples played a vital role in the classification process. A total of 165 randomly distributed land cover samples from May 20 to July 25, 2011, were used as training samples, including vegetation species, vegetation community structure, vegetation fraction, dominant vegetation species, and community structure. These samples are roughly homogeneous. The shrub sample size was set to 10 m × 10 m, and the herb sample size was 5 m × 5 m. A Garmin GPSMAP 60CSx was used to record the

Table 2 Characteristics of RapidEye images used in the present study

Imaging time	Level	Order number
2010-07-14	1B	2010-07-14T053310_RE2_1B-NAC_5833095_107072
2010-08-06		2010-08-06T053639_RE1_1B-NAC_5832782_107072
2010-08-18		2010-08-18T052536_RE4_1B-NAC_5833094_107072
2010-09-07		2010-09-07T052626_RE5_1B-NAC_4690511_98012
2010-09-09		2010-09-09T053018_RE2_1B-NAC_4298785_94549
2010-09-25		2010-09-25T052333_RE4_1B-NAC_4364240_95121

Table 3 Classification scheme of land use and land cover used in this study

No.	Classification	Description
1	Natural water	All areas of open water, including lakes and rivers
2	Salt marsh	Wetlands and regions of groundwater outflow
3	*Aeluropus littoralis*	Areas vegetated with *Aeluropus littoralis*, near spring outflow zones and marshes. It is noted that this species occurs in arid regions
4	Natural vegetation	Any plants or trees that grow on their own, without any form of human intervention, thus excluding *Aeluropus littoralis* (#3 above) and farmlands
5	Barren land	Bare exposed soil with less than 5 % vegetation, on plains of fine soil
6	Desertified land	Designated deteriorated land, with surface sand

longitude and latitude of each sample. In addition, the RapidEye image can help to determine training samples for classification. After the four images were classified, they were further smoothed based on a majority analysis with a 3 × 3 kernel. A total of 33 in situ survey samples were used for the accuracy assessment of LULC classification, and the results showed that the classification accuracy of MSS is the lowest (82.3 %) and the classification accuracy of TM in 2010 is the highest (90.6 %). Actually, the lower spatial resolution is not helpful to get the higher classification accuracy. However, its accuracy could meet with the requirement of this study.

Change detection method

Currently, there are a variety of change detection methods that are widely used to study LUCC. Thus, selecting an appropriate change detection method is increasingly vital for eco-environmental analysis. The post-classification comparison method provides "from–to" change information, and the types of LULC transformations that have occurred can be easily calculated (Sun et al. 2009). Furthermore, it has been widely proved to be the most effective approach for change detection, because each datum is classified separately, thereby minimizing the problem of normalizing for atmospheric and sensor differences between different dates (Jensen and Cowen 1999).

In this study, the post-classification comparison technique was applied to obtain the LUCC dataset for four intervals, namely 1975–1990, 1990–2000, 2000–2010, and 1975–2010.

Results and discussion

LULC classification and area change

The LULC maps for 1977, 1990, 2000, and 2006 are presented in Fig. 2. Furthermore, the area and changed areas of the six classes during the four intervals are shown in Table 4. It is evident that the area of barren land and desertified land has increased, while the natural vegetation area has declined continuously over the study period. From 1975 to 1990, the natural vegetation area declined from 3225.58 to 2304.86 km^2, a net decline of 920.72 km^2, which is the most rapid of the four intervals. This is consistent with the increase in bare land. Actually, the total increase in bare land was 995.3 and 586.29 km^2 of which occurred from 1975 to 1990. The area of desertified land was comparatively stable from 1975 to 1990 and then increased rapidly from 2000 to 2010, with a net increase of 77.18 km^2, up to 120.09 km^2, by 2010.

LUCC process

It is not enough just to know the area change over four intervals in order to analyze the eco-environment in the Dunhuang Basin. It is also necessary to calculate the change matrix of the LUCC to gain insight into internal transformations and future change patterns and trends (Table 5).

Natural vegetation

The area of natural vegetation in 1975, 1990, 2000, and 2010 was 3225.58, 2304.86, 2298.27, and 2010 km^2, respectively, representing a net decrease of 28.75 % (927.31 km^2) from 1975 to 2010. The largest decrease occurred from 1975 to 1990, when an area of 920.72 km^2, was turned into bare land, salt marshes, and *Aeluropus littoralis,* with areas of 558.24, 414.35, and 28.22 km^2, respectively. Despite the decrease in vegetation, the area change was smaller in 1990–2000; however, the area change was larger in 2000–2010. These results indicate that the natural vegetation in the study area had been degraded in the period 1975–2010, with the most serious degradation occurring in 1975–1990 and 2000–2010.

Figure 2 shows that the changes from natural vegetation to salt marsh occurred almost entirely in the western part of the study area, and the change from natural vegetation to barren land occurred mainly in the North Lake Natural Reserves.

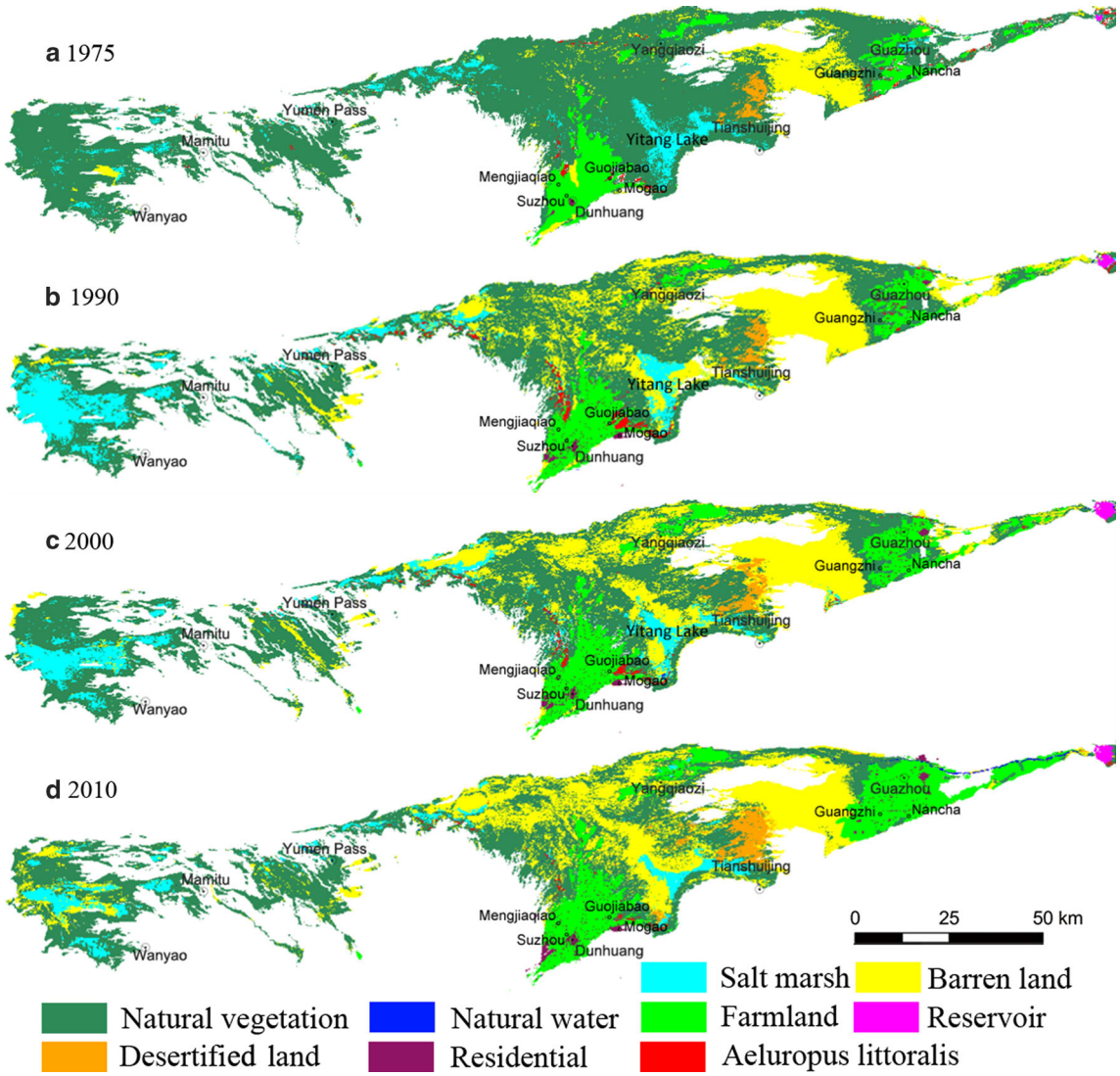

Fig. 2 Land use and land cover maps for four intervals

Table 4 Results of LULC classification in 1975, 1990, 2000, and 2010 showing area and area changed (km^2) of each class

Class	Area				Area changed			
	1975	1990	2000	2010	1975–1990	1990–2000	2000–2010	1975–2010
NV	3225.58	2304.86	2298.27	2101.16	−920.72	−6.59	−197.11	−1124.42
Barren land	88.5	674.79	801.43	1083.80	586.29	126.64	282.37	995.30
Salt marsh	226.73	545.52	418.57	288.20	318.79	−126.95	−130.37	61.47
Natural water	6.21	1.08	2.37	1.22	−5.13	1.29	−1.15	−4.99
AL	18.16	37.22	25.70	13.62	19.06	−11.52	−12.08	−4.54
DL	42.91	44.62	61.75	120.09	1.71	17.13	58.34	77.18

NV, natural vegetation; AL, *Aeluropus littoralis*; DL, desertification land

Bare land

The area of bare land in the study area increased from 88.5 km^2 in 1975 to 1083.8 km^2 in 2010 (Table 5), representing an increase of 1124 %. From Fig. 2, we can draw the conclusion that the spatial expansion of bare land was concentrated superjacent to the North Lake Natural Reserves and Wanyao and Mamitu, located in the West Lake National Natural Reserves.

Table 5 The change matrix of LULC from 1975 to 2010 in this present study (km^2)

	1975						1990 Total
	NV	Bare land	Salt marsh	Natural water	AL	DL	
(a) 1975–1990							
1990							
NV	2219.45	27.53	44.14	0.49	10.39	2.76	2304.76
Bare land	558.24	45.69	69.56	0.11	0.92	0.32	674.84
Salt marsh	414.35	13.77	111.94	4.90	0.54	0	545.5
Natural water	0.68	0.01	0.11	0.3	0	0	1.10
AL	28.22	1.49	0.84	0.41	6.31	0	37.27
DL	4.64	0.01	0.14	0	0	39.83	44.62
1975 Total	3225.58	88.5	226.73	6.21	18.16	42.91	3608.09
	1990						2000 Total
	NV	Bare land	Salt marsh	Natural water	AL	DL	
(b) 1990–2000							
2000							
NV	1883.11	225.88	171.06	0.33	14.51	2.57	2297.46
Bare land	332.61	401.16	57.39	0.09	0.22	10.5	801.97
Salt marsh	58.47	44.49	313.96	0.25	1.58	0.01	418.76
Natural water	0.32	0.03	1.42	0.40	0.22	0	2.39
AL	3.28	0.08	1.68	0.01	20.69	0	25.74
DL	27.07	3.15	0.01	0	0	31.54	61.77
1990 Total	2304.86	674.79	545.52	1.08	37.22	44.62	3608.09
	2000						2010 Total
	NV	Bare land	Salt marsh	Natural water	AL	DL	
(c) 2000–2010							
2010							
NV	1756.04	212.43	109.65	0.42	15.21	7.31	2101.06
Bare land	425.58	542.32	111.52	0.14	0.05	4.33	1083.94
Salt marsh	69.37	22.24	194.46	0.97	0.99	0.13	288.16
Natural water	0.11	0.02	0.28	0.80	0.02	0	1.23
AL	3.79	0.06	0.30	0.04	9.43	0	13.62
DL	43.38	24.36	2.36	0	0	49.98	120.08
2000 Total	2298.27	801.43	418.57	2.37	25.70	61.75	3608.09
	1975						2010 Total
	NV	Bare land	Salt marsh	Natural water	AL	DL	
(d) 1975–2010							
2010							
NV	2034.7	25.13	26.97	0.92	13.09	0.35	2101.16
Bare land	926.74	57.54	96.67	0.12	2.38	0.35	1083.8
Salt marsh	176.34	4.77	102.34	4.47	0.28	0	288.2
Natural water	0.36	0.03	0.06	0.69	0.08	0	1.22
AL	9.90	0.88	0.35	0.18	2.31	0	13.62
DL	75.6	0.04	2.24	0	0	42.21	120.09
1975 Total	3223.64	88.39	228.63	6.38	18.14	42.91	3608.09

NV, natural vegetation; AL, *Aeluropus littoralis*; DL, desertification land

The area of bare land increased from 88.5 km^2 in 1975 to 674.79 km^2 in 1990, of which 69.56 km^2 resulted from the conversion of salt marsh and 558.24 km^2 from natural vegetation. The area of bare land was 801.43 km^2 in 2000 and 1083.8 km^2 in 2010. It is obvious that the area increments are larger in both 1975–1990 and 2000–2010. This is consistent with the characteristics of the degradation of natural vegetation.

On the whole, the change in bare land tended to increase in the direction of vegetation → salt marsh → bare land. Furthermore, the conversion of salt marshes into bare land implies the decline of groundwater levels in the region. It is evident that the increased bare land mainly distributed in the three Lakes named West, North, and East Natural Reserves, respectively. This status is consistent with the decline of groundwater levels in some degree in the Dunhuang Basin.

Salt marsh

In 1975–1990, the salt marsh area increased from 226.73 to 545.52 km^2. During this period, 414.35 km^2 of natural vegetation had been changed into salt marsh, and 69.56 and 44.14 km^2 of salt marsh has been changed into bare land and natural vegetation, respectively. The salt marsh area was 418.57 km^2 in 2000 and decreased to 288.2 km^2 in 2010. The area has been declining since 1990. In the period 1990–2010, the declining salt marsh area mainly turned into bare land, indicating the decline of groundwater in the local region.

Figure 2 shows that the increased areas of salt marshes were mainly located in the West Lake National Nature Reserve, which originally consisted mainly of wetlands, with natural vegetation.

Natural water

In 1975, the area covered by natural water was 6.21 km^2, but declined to 1.08 km^2 in 1990. In 2000 and 2010, the areas covered by natural water were 2.37 and 1.22 km^2, respectively. The changes were smaller between 2000 and 2010; the natural water areas changed into 0.51 km^2 of salt marsh and 0.01 km^2 of bare land, and had totally disappeared by 2010. In 1975–2010, the change in total area of natural water showed no obvious pattern. This is because the seasonal features of surface water are difficult to capture with the snapshots acquired by remote sensing.

Desertified land

The change in area of desertified land was almost negligible between 1975 and 1990, from 42.91 to 44.62 km^2, respectively. However, from 2000, the area began to increase, covering an area of 61.75 km^2 by 2000. By 2010, desertified areas covered 120.09 km^2, of which 75.6 km^2 had been natural vegetation and 2.24 km^2 had been salt marsh. There was a net increase of 58.34 km^2. In the past 35 years, the increased desertified land mainly distributed on the east near the East Lake Natural Reserves.

Driving forces of LUCC

Drastic changes in surface water environment

First, the area of surface water vanished in the study area during the studying period. There are two large rivers running through the basin: the SuLe River in the northern part and the Dang River in the middle-southern part. However, in the 1960s, the surface water was dammed by three reservoirs, namely ShuangTa, ChangMa, and DangHe, resulting in nowadays the Sule River only flows temporarily at the upper reaches of the Dunhuang Basin; it dries out in the middle reaches and then re-emerges at the lower reaches because of groundwater discharge. The Dang River originates from the Qilian Mountains and is recharged by melting glaciers and snow, springs, and rainfall. In the southern edge of the basin, springs emerge in the mountains and flow out to form creeks that discharge to the groundwater in the basin (Sun et al. 2015).

From the classification results, the area of natural water during the dry season was 6.21 km^2 in 1975, but declined to 1.08 km^2 during the wet season in 1990. The water capacity downstream decreased and eventually dried up; oases degenerated or vanished; former traces of dried-up rivers, including the fine earth deposit of downstream lakes, suffered from wind erosion and turned into blow land; the river channels became sand dunes as a result. Meanwhile, the degeneration of vegetation strengthened wind erosion, accelerating the land desertification.

Actually LUCC occurred mainly in the center area of the three aforementioned Natural Reserves with great changes especially in natural vegetation and bare land, which are discharge area of shallow groundwater in the study area. The LUCC has a regular pattern, along with the development of groundwater recharge, runoff, and discharge conditions (Fig. 3). For example, farmlands expand outward, taking over natural oases; simultaneously, because of the changes in the water environment system, natural oases are changed into desertified land; salt marshes emerged with the changes in groundwater discharge; finally, desertification occurs by weathering; at the same time, wetlands and lakes around the springs shrink and vanish. These results indicate that the groundwater flow system (GFS) in the study area is the key factor controlling the changes in LULC.

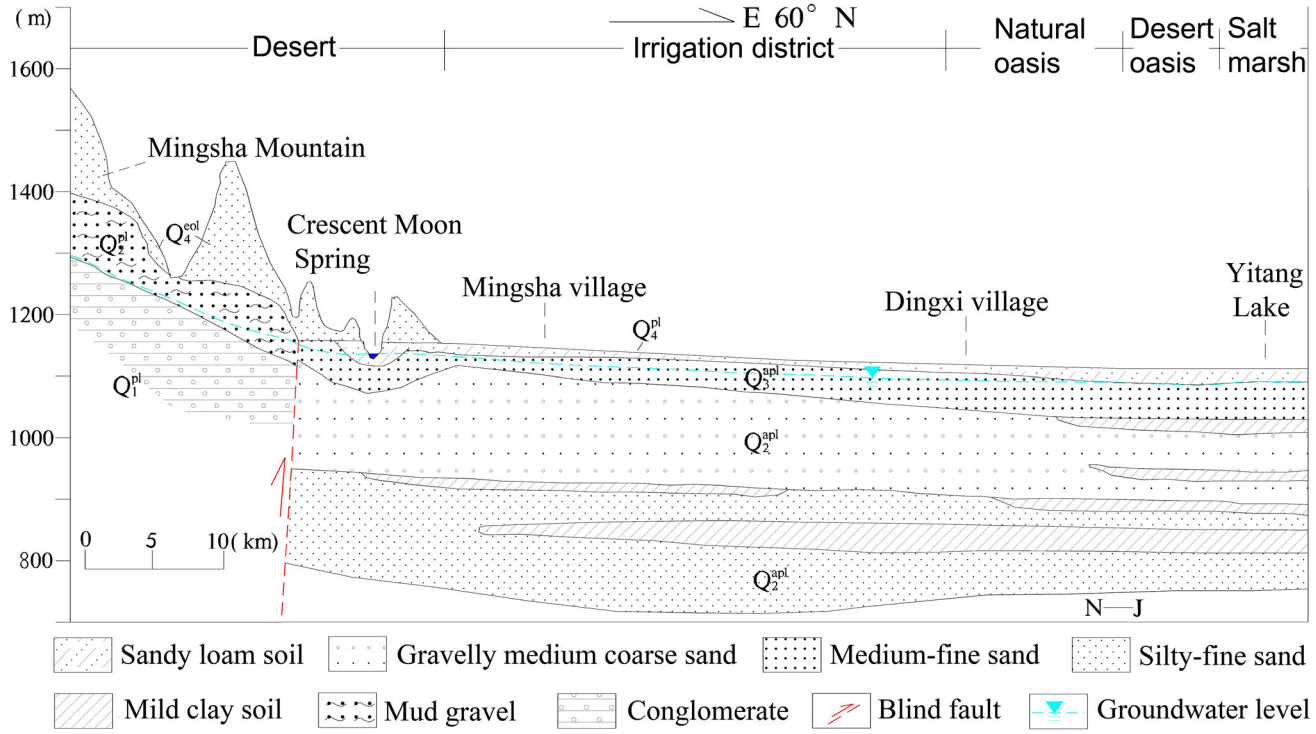

Fig. 3 The spatial relationship between local hydrogeological section and land use/land cover in the study area

Large-scale reclamation of farmland and greater groundwater pumping

According to the results of image interpretation in this study, farmland areas in 1975, 1990, 2000, and 2010 covered 490, 531.23, 690.93, and 929.56 km^2, respectively. The increase in area farmlands over 35 years reached 439.56 km^2. Furthermore, most of the farmlands from 1990 to 2010 consisted of cash crops such as Hami melon, grape, and cotton. These crops require a large quantity of water, most of which is extracted from the groundwater supply. Artificial extraction of groundwater was conducted mainly in the farmlands. Especially after the implementation of comprehensive development projection in Sule River watershed, immigration relocated to the projection area and resulted in rapidly extension of farmlands and the volume of extraction of groundwater. This greatly affected the inflow of groundwater and surface water. According to data from the institute of China's Gansu geo-environment monitoring, the evapotranspiration in the study area was 4.51×10^8 m^3 in 1977, 4.65×10^8 m^3 in 1999, both 3.61×10^8 m^3 in 2004 and 2008. In addition, the net extraction volume of groundwater was 3.13×10^7 m^3 in 1977, 5.88×10^7 m^3 in 1999, 1.08×10^8 m^3 in 2004, and 1.81×10^8 m^3 in 2008. It is evident that there was a great increase in groundwater extraction within 30 years.

In addition, continued expansion of farmlands has destroyed and disturbed the inherent properties of the ground surface and geomorphology, forming new sand dunes and small-sized wind erosion lands. Furthermore, in order to improve groundwater utilization, irrigation channels are often made resistant to water seepage. Thus, the groundwater level is constantly decreasing. Meanwhile, recharge from surface water is becoming more and more difficult.

According to data from the institute of China's Gansu geo-environment monitoring, the groundwater level has been actually declined with different extent within the Dunhuang Basin. The most declined region occurred at the puluvial fan, followed by the transition zone between the puluvial fan and the oasis, and the oasis had the smaller decline. In addition, according to the monitoring data of groundwater level twice per year in the Danghe irrigation area from 2008 to 2010, the declined range of 0.10–0.50 m/a was mainly occurred from Suzhou town to Mengjiaqiao town and the Northeastern Mogao town; the declined range of 0.10–0.30 m/a was mainly distributed from Zhuanqukou, Guojiabao to Mogao town and around them; the declined range of 0.10–0.20 m/a was mainly distributed in the south of the Dunhuang irrigation area and other districts. Furthermore, in Guangzhi and Nancha town along the south of Guazhou irrigation area, the groundwater level has been almost declining. For example, since 1996 the

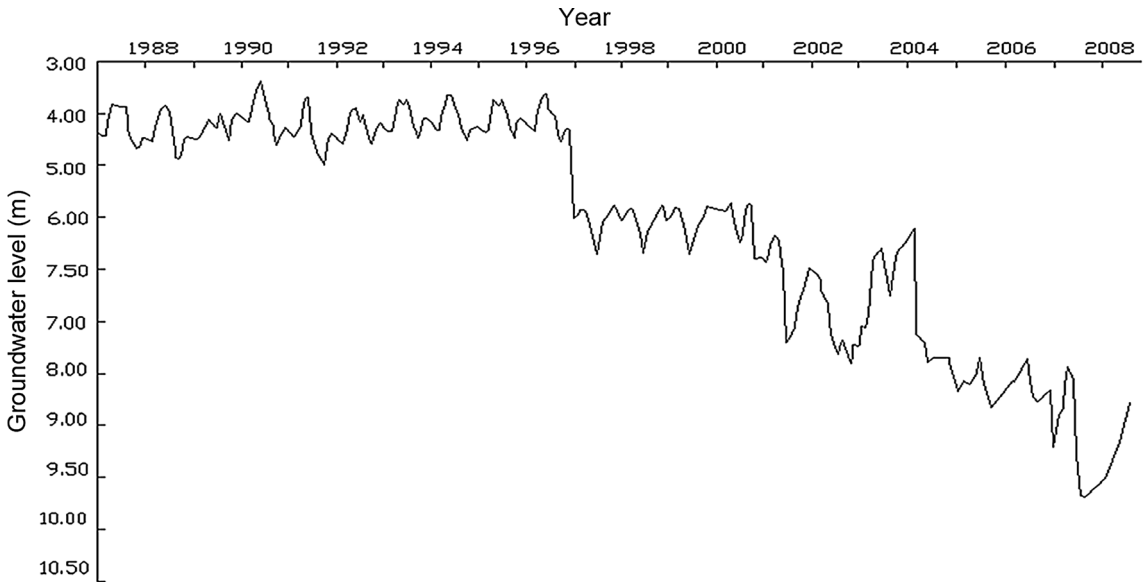

Fig. 4 A change profile of groundwater level in point *N* around recent 30 years

Table 6 Changes of climate factors in Dunhuang Basin from 1971 to 2010 (modified from Song et al. 2014)

Period	Mean annual temperature (°C)	Annual precipitation (mm)	Mean annual wind velocity (m/s)
1971–1980	9.23	51.56	2.47
1981–1990	9.41	35.45	1.92
1991–2000	9.88	39.63	1.75
2001–2010	10.61	52.06	1.33

decline range of point N presented in Fig. 1 was gradually from 0.95 to 11.07 m (Fig. 4).

Local climate factors have also had an increasing impact on LUCC in the Dunhuang Basin. According to observations (Song et al. 2014), the mean annual temperature and annual precipitation from 1971–2010 changed greatly, with the former generally increasing, while the latter declined, contributing to the increased desertification. In addition, overgrazing has worsened the effect of the land cover change (Table 6).

Conclusions

The Dunhuang Basin has been increasingly importance for the ecological safety of northwestern China. LULC and LUCC, including natural water, salt marshes, *Aeluropus littoralis,* natural vegetation, barren land, and desertified land, were analyzed based on RapidEye and four temporal Landsat images in the present study. Furthermore, the key driving forces were analyzed focused on the changes of water environment system and human activities. Some remarkable conclusions can be drawn as follows.

Over the past around 35 years, the LUCC in the Dunhuang Basin made great changes. The area of barren lands and desertified lands increased, while areas of natural vegetation declined continuously. The rate of decline of natural vegetation was the most rapid within 1975–1990. This was consistent with the increase in bare land. Furthermore, the area of desertified land increased greatly from 2000 to 2010. Vegetation degeneration turning into bare land is one of the main problems. What is more, wetlands have been shrinking rapidly; spring lakes have been almost stable over the past 20 years, but decreased rapidly from 1975 to 1990, many of them degenerating into salt marshes and then vanishing. The area of hydrophilic vegetation (*Aeluropus littoralis*) has also decreased. Salt marsh areas have continuously decreased and gradually degenerated into saline and alkaline lands, and bare land. In contrast, the area of bare land has increased continuously, indicating not only the degeneration of vegetation or wetlands, but also presenting a key format of land degeneration in the Dunhuang Basin. In addition, desertified land has continually increased, which is closely related to the decrement of groundwater levels and degeneration of vegetation. These can reveal that the eco-environment of the Dunhuang Basin presents a severely worsening trend.

The water environment system is the most key factor contributing to the LUCC over the past around 35 years. The surface water environment is still destructive because three reservoirs, including ShuangTa, ChangMa, and DangHe, impede the surface water from supplementing soil and vegetation. Thus, how to effectively allocate surface water resources for the Sule River and Dang River is worth

to attract more attention. In the future, it is very important to achieve the balance between meeting with the ecology water demanding and avoiding salinization. In addition, inappropriate human activities including extensive commercial farmlands reclamation and greater groundwater pumping could contribute to the rapid LUCC in the Dunhuang Basin. Thus, it is necessary to build up optimizing model of water resources especially for the Dunhuang Basin in the future work.

Acknowledgments The research was supported jointly by the Fundamental Research Funds for the Central Universities, China University of Geosciences (Wuhan) (No. CUGL150417), Foundation for Innovative Research Groups of the National Natural Science (No. 41521001), and the China Scholarship Council (No. 201406415051). We wish to thank Kong Lingfeng, Zhao Duohui, Liu Bo, and Yan Zezhou for helping to conduct out the in situ training sampling investigation. We also wish to thank reviewers for the comments.

References

Atkinson PM, Tatnall ARL (1997) Introduction neural networks in remote sensing. Int J Remote Sens 18:699–709

Benediktsson JA, Swain PH, Ersoy OK (1990) Neural network approaches versus statistical methods in classification of multisource remote sensing data. IEEE Trans Geosci Remote Sens 28:540–552

Couturier S, Gastellu-Etchegorry JP, Patino P, Martin E (2009) A model-based performance test for forest classifiers on remote-sensing imagery. For Ecol Manag 257(1):23–37

de Freitas MWD, dos Santos JR, Alves DS (2013) Land-use and land-cover change processes in the Upper Uruguay Basin: linking environmental and socioeconomic variables. Landsc Ecol 28:311–327

Fisher PF (2010) Remote sensing of land cover classes as type 2 fuzzy sets. Remote Sens Environ 114:309–321

Foley JA, DeFries R, Asner GP, Barford C, Bonan G, Carpenter SR, Chapin FS, Coe MT, Daily GC, Gibbs HK et al (2005) Global consequences of land use. Science 309:570–574

Foody GM (2010) Assessing the accuracy of land cover change with imperfect ground reference data. Remote Sens Environ 114:2271–2285

Gong B, Im J, Mountrakis G (2011) An artificial immune network approach to multi-sensor land use/land cover classification. Remote Sens Environ 115:600–614

Hagner O, Reese H (2007) A method for calibrated maximum likelihood classification of forest types. Remote Sens Environ 110:438–444

Hüttich C, Herold M, Wegmann M, Cord A, Strohbach B, Schmullius C, Dech S (2011) Assessing effects of temporal compositing and varying observation periods for large-area land-cover mapping in semi-arid ecosystems: implications for global monitoring. Remote Sens Environ 115:2445–2459

Jensen JR, Cowen DC (1999) Remote sensing of urban/suburban infrastructure and socio-economic attributes. Photogramm Eng Remote Sens 65:611–622

Li F, Xu Z, Feng Y, Liu M, Liu W (2013) Changes of land cover in the Yarlung Tsangpo River basin from 1985 to 2005. Environ Earth Sci 68:181–188

Lira PK, Tambosi LR, Ewers RM, Metzger JP (2012) Land-use and land-cover change in Atlantic Forest landscapes. For Ecol Manag 278:80–89

Liu JY, Deng XZ (2010) Progress of the research methodologies on the temporal and spatial process of LUCC. Chin Sci Bull 55:1–9

Lunetta RS, Elvidge CD (1998) Remote sensing change detection: environmental monitoring methods and applications, 1st edn. Ann Arbor Press, Chelsea

Ma J, He J, Qi S, Zhu G, Zhao W, Edmunds WK, Zhao Y (2013) Groundwater recharge and evolution in the Dunhuang Basin, northwestern China. Appl Geochem 28:19–31

Ni J, Shao J (2013) The drivers of land use change in the migration area, Three Gorges Project, China: advances and prospects. J Earth Sci 24:136–144

Pérez-Hoyos A, García-Haro FJ, San-Miguel-Ayanz J (2012) A methodology to generate a synergetic land-cover map by fusion of different land-cover products. Int J Appl Earth Obs Geoinf 19:72–87

Rogan J, Chen DM (2004) Remote sensing technology for mapping and monitoring land-cover and land-use change. Prog Plan 61:301–325

Sang X (2006) Visual Simulation and management of groundwater in Dunhuang Basin. Master's thesis, Lanzhou University, Lanzhou, China **(in Chinese)**

Seeber C, Hartmann H, Xiang W, King L (2010) Land use change and causes in the Xiangxi catchment, Three Gorges Area derived from multispectral data. J Earth Sci 21(6):846–855

Song X, Yan CZ, Li S, Xie JL (2014) Assessment of sandy desertification trends in the Shule River Basin from 1978 to 2010. Sci Cold Arid Reg 6(1):52–58

Stavrakoudis DG, Galidaki GN, Gitas IZ, Theocharis JB (2010) Enhancing the interpretability of genetic fuzzy classifiers in land cover classification from hyperspectral satellite imagery. IEEE international conference on fuzzy systems (FUZZ), Barcelona, Spain

Stavrakoudis DG, Theocharis JB, Zalidis GC (2011) A boosted genetic fuzzy classifier for land cover classification of remote sensing imagery. ISPRS J Photogramm Remote Sens 66:529–544

Sun Z, Ma R, Wang Y (2009) Using Landsat data to determine land use changes in Datong basin, China. Environ Geol 57:1825–1837

Sun Z, Ma R, Wang Y, Hu Y, Sun L (2015) Hydrogeological and hydrogeochemical control of groundwater salinity in an arid inland basin: Dunhuang Basin, northwestern China. Hydrol Process. doi:10.1002/hyp.10760

Tang J, Lin N (1995) Some problems of ecological environmental geology in arid and semiarid areas of China. Environ Geol 26:64–67

Turner BL, Lambin EF, Reenberg A (2007) The emergence of land change science for global environmental change and sustainability. Proc Natl Acad Sci USA 104:20666–20671

Volpi M, Tuia D, Bovolo F, Kanevski M, Bruzzone L (2013) Supervised change detection in VHR images using contextual information and support vector machines. Int J Appl Earth Obs Geoinf 20:77–85

Wang X (2009) A study on desertification based on RS and GIS in Dunhuang city. Master's thesis, Lanzhou University, Lanzhou, China **(in Chinese)**

Zhang M, Zhao Z, Zeng Z (2003) The characteristics of water system and the sustainable utilization of water resources in Dunhuang Basin. J Arid Land Resour Environ 17:71–77 **(in Chinese)**

Zhang X, Zhang L, He C, Li J, Jiang Y, Ma L (2014) Quantifying the impacts of land use/land cover change on groundwater depletion in Northwestern China—a case study of the Dunhuang oasis. Agric Water Manag 146:270–279

Zhao R, Chen Y, Shi P, Zhang L, Pan J (2013) Land use and land cover change and driving mechanism in the arid inland river basin: a case study of Tarim River, Xinjiang, China. Environ Earth Sci 68:591–604

View publication stats